Thermochimica Acta 488 (2009) 66–77

Contents lists available at ScienceDirect

Thermochimica Acta

journal homepage: www.elsevier.com/locate/tca

Performance investigation of high-temperature heat pumps with various BZT working fluids

C. Zamfirescu*, I. Dincer

Faculty of Engineering and Applied Science, University of Ontario Institute of Technology (UOIT), 2000 Simcoe Street North, Oshawa, ON, Canada L1H 7K4

ARTICLE INFO

Article history:
Received 13 October 2008
Received in revised form 26 January 2009
Accepted 27 January 2009
Available online 5 February 2009

Keywords:
Non-classical gas dynamics
BZT effects
High-temperature heat pumps
Renewable energy

ABSTRACT

In this paper we propose four kinds of high-temperature heat pumps with mechanical compression, working with various Bethe–Zel'dovich–Thompson (BZT) fluids, and study their performances for comparison purposes. A total of 17 molecularly complex fluids from the class of siloxanes and perfluorocarbons are selected as potential working fluids. The Martin–Hou, Peng–Robinson–Stryjek–Vera and Span–Wagner equations of state are used in the analysis. A parametric study is also conducted for a range of isentropic efficiency and temperatures at sink and source. The results of the energetic and exergetic coefficient of performances show that the heat pumps proposed in this study appear to be attractive for some applications with a temperature difference of about 50 °C, whenever heat and/or work recovery, or using a non-conventional energy source (renewable, waste heat, waste matter) or sustainable nuclear energy is possible. Examples of such applications may include providing heat to high-temperature endothermic reactions, thermo-chemical water splitting, physical processes (e.g., distillation), or industrial heat treatments. Among the fluids studied here, siloxanes show the best performance.

1. Introduction

Studying the behaviour of supersonic flows is of great importance in turbomachinery design and applications. In general, turbo-compressors are designed in such a way that there is no supersonic flow in the rotor to avoid shock formation and the associated irreversibility losses. The turbines with supersonic discharging nozzles must be designed such that shocks do not occur either in stator or in rotor where the flow is recompressed due to the impact with the rotating blades. Because turbomachinery are key elements in energy conversion cycles, improving their performance is of actual interest, especially when they are used in applications exploiting non-conventional energy sources.

Furthermore, understanding the behaviour of gas dynamic waves appears to be essential for turbomachinery design and performance assessment. The behaviour of gas dynamics waves is basically defined through the curvature of isentropes in P–v diagram, i.e., the sign of $(\partial^2 P/\partial v^2)_s$, where P is pressure, v specific volume and "s" indicates constant entropy. If $(\partial^2 P/\partial v^2)_s > 0$, the curvature is positive – that is the isentropes are convex in P–v diagram; this is the common case encountered in practice. To give an example, the isentrope 7–8 shown in Fig. 1 at scale in reduced coordinates (index r) for a polytropic Van der Waals fluid, becomes convex.

It is demonstrated theoretically that fluids composed of molecules of sufficient complexity may display isentropes that are concave in the P–v thermodynamic diagram – that is, have negative curvature, i.e., $(\mathrm{d}^2 P/\mathrm{d}v^2)_s < 0$ – in a limited region on the vapour side, in the vicinity of the critical point [1]. As a consequence, it is physically possible that supersonic waves evolving in that region behave in a counter-intuitive fashion: compressions are smooth and isentropic while expansions are steep and non-isentropic. These effects, which are explained in more detail in the next section, may be exploited in designing turbomachinery for better efficiency and compactness.

The first reference to these phenomena is due to Bethe [2] who investigated shock waves caused by nuclear explosions with other equation of state (EoS) than that of ideal gas. Bethe [2] basically used the Van der Waals equation of state and found that for fluids characterized with a specific heat higher than a threshold value, there is a kind of limited thermodynamic region where the isentropes are concave.

Later, the theory of Bethe was confirmed by the more thorough analyses of Zel'dovich [3] and Thompson [4] that show that the negative curvature region is a fundamental property of complex fluids, independent on the adopted EoS. The related phenomena and the complex fluids that support them are known nowadays as BZT, from the names of the three researchers who pioneered the field. Up to present date few organic compounds belonging to class of alkanes, ethers, perfluorocarbons and siloxanes are identified as being BZT fluids [5]. The thermodynamic region where non-classical gas dynamics phenomena can manifest is known as BZT region.

* Corresponding author.
E-mail addresses: Calin.Zamfirescu@uoit.ca (C. Zamfirescu), Ibrahim.Dincer@uoit.ca (I. Dincer).

0040-6031/$ – see front matter © 2009 Elsevier B.V. All rights reserved.
doi:10.1016/j.tca.2009.01.028

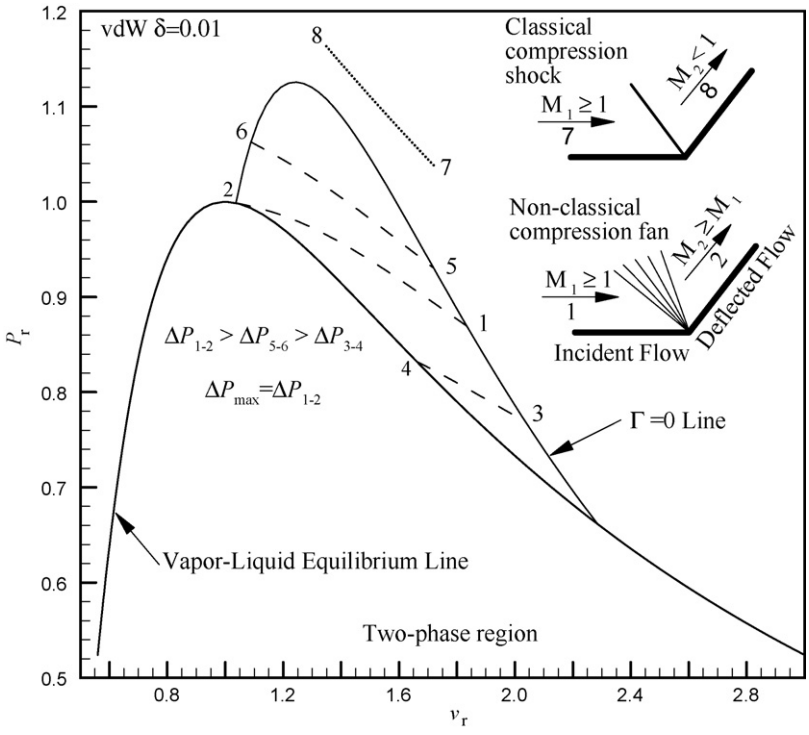

Fig. 1. Non-classical flow field over a compression corner.

As stated by Kluwick [1], efforts have been exerted in the open literature to characterize BZT phenomena (known also as "non-classical" gas dynamics). These refer mainly to characterizing the flow fields and determining the thermodynamic conditions for such effects to occur. Hayes [6] introduced a thermodynamic parameter called the fundamental derivative of gas dynamics, which is a thermodynamic property of any substance that characterizes the behaviour of gas dynamic waves that it supports. This property is defined by

$$\Gamma \equiv \frac{v^3}{2c^2}\left(\frac{\partial^2 P}{\partial v^2}\right)_s \tag{1}$$

where v is the specific volume, P is the pressure and $c^2 = -v^2(\partial P/\partial v)_s$ is the zero-frequency speed of sound.

A fluid to be BZT has to have a thermodynamic region where Γ is negative. As demonstrated by Thompson [4], this region coincides with the above mentioned one where the isentropes are concave in the P–v diagram. It has been recently demonstrated a procedure to determine the extent of the thermodynamic region where BZT effects may manifest, independent on the adopted fluid model [7]. This thermodynamic region includes the $\Gamma < 0$ region. Moreover, it has been shown that there is a superior limit of the intensity of non-classical expansion shock waves that can be expressed in terms of wave Mach number, or pressure drop, or shock strength [8]. The thermodynamic states behind and over the non-classical wave with maximum intensity can be predicted and are unique for any given fluid [9].

The accuracy of the adopted EoS is essential in predicting the pre-shock and post-shock states. Starting with the pioneering work of Lambrakis and Thompson [10], numerous research efforts have been spent to produce or collect experimental data for complex molecule fluids believed to display BZT effects and to develop accurate fluid models (e.g., [11,12]).

An example of recently developed EoS is due to Nannan et al. [13] which measured the sound-speed in octamethylcyclotetrasiloxane (D_4) and then extrapolated the data with ab-initio calculations to a number of dimethylsiloxanes. The result of this work is represented by a highly accurate "technical" equation of state [14] that predicts that five fluids from the class of siloxanes are BZT. The list may be expanded with more complex fluids from the same class (for which an accurate EoS is not yet available).

Among the investigated fluids, siloxanes received special attention because of their favourable characteristics for energy conversion applications – non-toxic, good lubricating, thermo-chemically stable at high-temperatures with low flammability. In the case of organic Rankine cycle (ORC) applications, these compounds exhibit good thermophysical properties with respect to cycle design (e.g., [15,16]). Moreover, siloxanes are bulk-produced, mainly for the cosmetics industry.

Several studies investigated with advanced computational fluid dynamics (CFD) codes and accurate equation of state the behaviour of non-classical flow fields over various geometries. In the study by Colonna and Rebay [17] that adopts the Peng–Robinson [18] EoS as modified by Stryjek and Vera [19] and uses the group's CFD software zFlow [20], it is shown that if the upstream state is appropriately chosen in the vicinity of the non-classical thermodynamic region, a BZT two-dimensional flow field displays expansion shocks.

Brown and Argrow [21] also show that a non-classical flow over turbine cascades may be such that improves the turbine efficiency with up to 3% with respect to classical flow fields counterparts, due to diminishing of shocks and boundary layer detachment occurrence. In fact, in a previous paper Brown and Argrow [22] show that the obtained flow fields in the non-classical dense gas region are different from the two-dimensional flow fields if the fluid is a perfect gas. Brown and Argrow used the Van der Waals EoS that even if is incapable of accurately predicting thermodynamic properties in the dense gas region, it does however describe the fluid correctly from a qualitative point of view.

Some studies, as reviewed by Zamfirescu et al. [23], attempting to experimentally generate and record BZT effects were also reported in the literature. However, as mentioned in Zamfirescu et al. [24] there is no successful measurement to date of non-classical flow fields. Some recent efforts by the group of Colonna [25,26] have

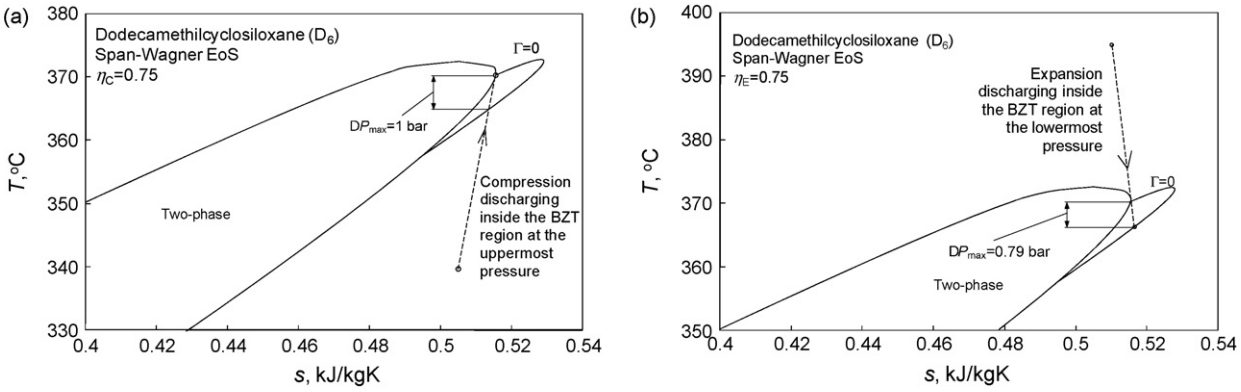

Fig. 2. Compression (a) and expansion (b) processes with discharge inside the BZT region.

focused on the development of a peculiar high-temperature shock tube technique aimed at generating and measuring non-classical flow fields. The results of their advanced analytical and numerical simulation of the experiment (and other turbomachinery simulations [27]) suggest that the proposed technique, involving a special high-temperature fast opening valve, operates within technological limits. Therefore they expect that once the experiments are started a first measurement and evidence of the non-classical phenomena will be obtained.

In parallel with the works aiming at the experimental investigation and fundamental/theoretical developments in non-classical gas dynamics, some published studies are concerned with the application of BZT effects. One may suggest exploiting BZT phenomena in some process engineering applications where, e.g., rapid cooling can be obtained in a shock tube device behind a travelling rarefaction shock wave. However, the cited application up to present date refers to organic Rankine cycles where the BZT fluid can be expanded in a shock-free turbine with high efficiency. The works done by Colonna et al. [27] and Cinnella and Congedo [28] are relevant in this regard.

In fact, a turbo-compressor running within BZT region may operate shocks-free even for slightly supersonic flows and favours the possibility of developing high-temperature heat pumps where heat is upgraded from a lower to a higher temperature by work conversion during a compression process. This paper investigates the possibility of developing heat pumps equipped with turbomachinery (turbines or compressors) that exploit BZT effects for better performance and compactness. Moreover, the envisaged applications are in the field of so called "green energy", because by using heat pumps, heat and work recovery can be applied and fossil fuel use reduced with positive impact on the environment.

The primary purpose of this paper is to propose some potential BZT type working fluids for utilization in heat pumps with mechanical compression and study their performance comprehensively through thermodynamic analysis. In the parametric study performed in this paper we assume isentropic efficiency between two extremes and study the heat pump efficiency with 17 BZT fluids. The lowest bound of the isentropic efficiency is taken as 0.7 based on the practical experience with axial turbo-compressors for gas turbines that can attain efficiency over 0.85. The highest bound becomes one which represents the ideal case of an isentropic process. The paper is structured to discuss the exploitation of BZT effects in turbomachinery and some available BZT fluids and EoS, propose four potential heat pump cycles, and include a performance modeling and their comparisons for various cases.

2. Potential working fluids with BZT effects

In industry there are numerous thermo-chemical processes involving endothermic chemical reactions with heat input, particularly in chemical and petrochemical processes and renewable energy sector. A potential example is hydrogen production via thermo-chemical water splitting [29]. The nuclear process heat is used as a heat source to drive the thermo-chemical reactions for water splitting purpose, as proposed recently, for example, through the Cu–Cl cycle [30].

A proposed solution for upgrading the temperature level of the heat generated by the nuclear reactor is presented in [31,32]. A chemical heat pump is integrated with the secondary Rankine cycle loop of a supercritical water-cooled nuclear reactor. Steam is combined with methane while providing heat from the nuclear reactor as a first step, and the reverse exothermic methane synthesis reaction is conducted at a higher temperature as the second step. The two steps are repeated cyclically. Water splitting is obtained through Cu–Cl cycle which is driven by a high-temperature synthesis heat of methane. Some work is consumed from the Rankine

Table 1
BZT working fluids for high temperature heat pumps.

Fluid	D_4	D_5	D_6	MD_3M	MD_4M	MD_5M	MD_6M	PP_5	PP_9
EoS	PRSV	PRSV	SW	SW	SW	PRSV	PRSV	PRSV	MH
M_m (kg/kmol)	0.297	0.371	0.445	0.385	0.459	0.533	0.607	0.462	0.512
T_c (°C)	313.4	346.0	372.7	355.2	380.1	398.7	415.8	291.9	313.4
P_c (bar)	13.3	11.6	9.6	9.5	8.8	7.6	6.8	17.9	16.8

Fluid	PP10	PP11	PP24	PP25	D5-D6	MD_2M-MD_3M	MD4M-MD5M	MD5M-MD6M
EoS	MH	MH	MH	MH	PRSV	PRSV	PRSV	PRSV
M_m (kg/kmol)	0.574	0.624	0.686	0.774	0.408	0.348	0.496	0.570
T_c (°C)	357.0	377.0	428.1	400.5	360.0	340.0	389.0	407.0
P_c (bar)	16.4	14.6	15.3	11.5	10.6	10.0	8.2	7.2

MH: Martin–Hou [50]; PRSV: Penrg–Robinson–Stryjek–Vera [20]; SW: Span–Wagner [49]. The short notations of the fluids are the ones used in [5] and [47]. M_m: molecular mass, T_c, P_c: critical temperature and pressure, respectively.

turbine shaft to drive a compressor having the role to shift the chemical equilibrium in the desired direction, by adjusting the reaction pressure.

Many other types of chemical heat pumps, which generally use turbomachinery for shifting the chemical equilibrium through regulation of the reaction pressure, are presented in the open literature [33–38]. Apart from chemical heat pumps, vapour compression and absorption heat pumps are also considered for various high-temperature applications, such as drying [39], distillation [40,41], pasteurization [42], steam generation [43,44], etc.

A vapour compression heat pump consumes some shaft work to compress a working fluid to the desired temperature level. The

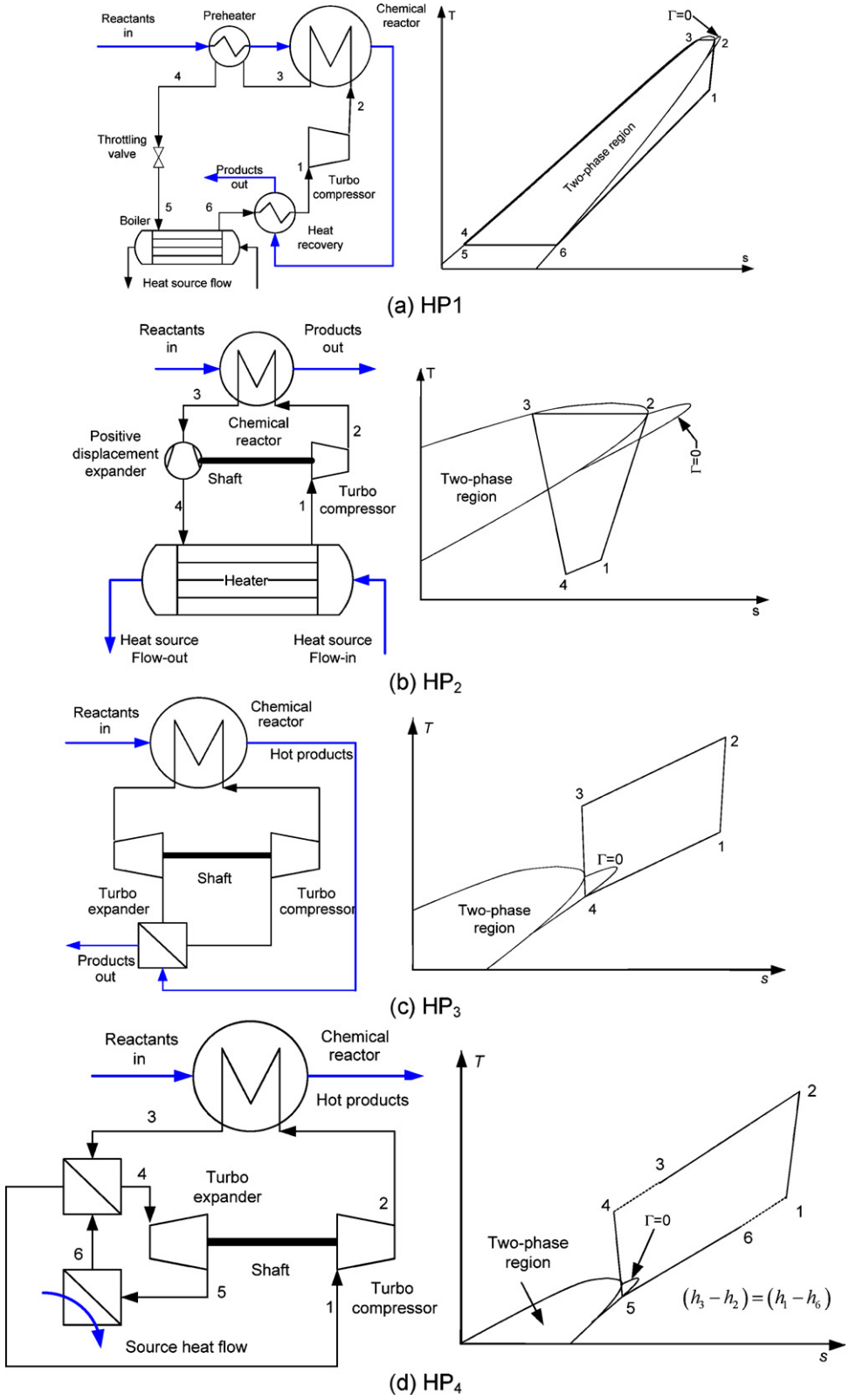

Fig. 3. Four potential heat pump cycles studied.

heat is thereafter delivered to a heat exchanger or high-temperature chemical reactor to serve as energy input for a desired process. Apart from the ability of "capturing" and upgrading heat from non-conventional and/or clean energy sources, a mechanically driven heat pump better matches the temperature profile at sink and source in the favour of improved exergy efficiency. This is a real advantage over the classical non-clean fossil fuel combustion with a heat recovery option as demonstrated in [45].

In this section relevant fundamental aspects of non-classical gas dynamics–relevant to turbomachinery employed in vapour compression heat pumps – are analyzed, and the main parameters characterizing such phenomena are presented for a number of candidate BZT fluids.

As shown in detail by Zamfirescu et al. [24] the following relationship (derived based on the Maxwell equations) is valid in any substance

$$\left(\frac{\partial P}{\partial v}\right)_s = \left(\frac{\partial P}{\partial v}\right)_T - \frac{T}{C_v}\left(\frac{\partial P}{\partial T}\right)_v^2 \quad (2)$$

which yields, in the limit of fluids with complex molecule featuring high specific heat, i.e., when $C_v \to \infty$, that the isentropes approach the isotherms. Here T stands for temperature and C_v for specific heat at constant volume. Because for any fluid the isotherms are concave in the vicinity of critical point it follows that, for complex molecule fluids, isentropes are also concave in about the same thermodynamic region.

Based on this fundamental observation one concludes that some complex fluids may be BZT. For more reference on the possible non-classical waves the reader is referred to Zamfirescu et al [7]. Here we briefly discuss one of the most intriguing BZT effects, namely generating smooth and isentropic waves over compression corners.

In Fig. 1 one presents the P–v diagram in reduced coordinates of a polytropic Van der Waals fluid having the specific heat given in the dimensionless form $\delta = R/C_v = 0.01$. Analytical expressions for the thermal and caloric forms of Van der Walls equation, the saturation line and $\Gamma = 0$ locus can be found e.g., in [46]. The $\Gamma = 0$ locus represents the boundary of the region where Γ is negative, i.e., where the isentropes become concave.

Let us assume now that this fluid is in the thermodynamic state indicated with 1 in the diagram, which is on the $\Gamma = 0$ line. Moreover, the fluid has a slightly supersonic speed. Now, if the flow passes over a compression ramp – as suggested in Fig. 1 (indicated with "non-classical compression fan") – it will be subjected to acceleration due to the negative curvature of the isentropes. The flow thus will not display shocks and will evolve isentropically. Outside the non-classical compression fan the flow is parallel to the deflecting surface and has the same entropy as at 1.

Among all possible downstream states, the state indicated with 2, at the intersection of $\Gamma = 0$ with vapour liquid equilibrium (VLE) line corresponds to the isentropic compression evolving in vapour phase with maximum pressure difference across. In the figure this is indicated with ΔP_{max}, where $\Delta P_{max} = \Delta P_{1-2} > \Delta P_{5-6} > \Delta P_{3-4}$ and 3, 4, 5, 6 indicate states connecting other possible upstream and downstream states of compression fans. Note that in Fig. 1 it is also illustrated, for comparison purpose, the flow field 7–8 of an oblique shock over compression corner, situation in which the flow decelerates to subsonic speed.

With the above analysis, we may contemplate the design of a turbo-compressor operating with BZT fluid. Since in the turbo-compressor the fluid flows always against an adverse pressure gradient one has, as mentioned in the introduction, to take precaution that the flow is always subsonic in the rotating reference frame, so that no shocks may occur. The peculiarity of BZT fluids allows higher compression ratios – as compared to regular fluids – corresponding to even slightly supersonic flows discharging inside the non-classical region. Moreover, a turbo-compressor that will discharge in a state close to state 2 will benefit the most from the BZT effects for improving efficiency and decreasing the needed number of stages, i.e., increasing the compactness.

Another feature of the BZT fluids is represented by their retrograde character. A retrograde fluid presents a vapour saturation line with positive slope in the T–s diagram. As a consequence, both compression and expansion processes are facilitated. In Fig. 2 one represents the VLE and $\Gamma = 0$ locus in the T–s diagram of dodecamethylcyclohexasiloxane, having the short name D_6, and the chemical formula $((CH_3)_2SiO)_6$. The Span–Wagner [48] EoS implemented in the FluidProp software [47] has been used for calculations. In Fig. 2(a) it is presented with dashed line a compression process that proceeds from 1 bar pressure with an isentropic efficiency of 75%, and discharges at the extreme upper pressure inside the non-classical region. If a turbo-compressor operates according to this process the BZT effects will be benefited at maximum. In Fig. 2(b) it is illustrated an expansion process that never crosses the two-phase region, but touches the VLE line at one single point and discharges at the lowest pressure inside the BZT region. This is the case of a typical BZT turbine where if one discharges at the lowest pressure inside the BZT region one can diminish the risk of shock formation due to the recompression of the supersonic flow at the impact with the rotor blades. Rather this local recompression evolves isentropically in this case.

In summary, with BZT fluids the expansion and compression processes are facilitated first due to their retrograde character. Secondly, if the thermodynamic states upstream and downstream of turbomachine are well chosen (as indicated, e.g., in Fig. 2) the risk of shock formation is diminished and moreover enhanced compression/expansion efficiency and higher compactness could be achieved. However, boundary layer detachment may still occur, especially in compressors, due to other gas dynamic processes (including turbulence and boundary layer growth) and this obviously induces irreversibilities. In Fig. 2 there is also indicated the value of the ΔP_{max} defined above, which in the case of the fluid D_6 is of the order of 1 bar for compressors and 0.79 bar for expanders.

Three kinds of EoS are used in this paper for modeling 17 BZT fluids selected from the class of siloxanes and perfluorocarbons, namely those of Span and Wagner (SW) [48], of Stryjek and Vera (PRSV) [19], and of Martin and Hou (MH) [49]. All state equations used have fluid specific fitting parameters as developed in earlier works [5,12–15]. The critical properties and the used equation of state for the fluids investigated herein are indicated in Table 1. The selection of the equation of state is based on the availability and accuracy. As an example, for D_6 one disposes of three EoS, namely MH, PRSV, and SW. In this case the chosen equation has been the SW because it is the most accurate amongst all. For PP_5 there are available both MH and PRSV equations and one employs the PRSV. According to former recommendations [8,9] the SW EoS is the most and MH is the least accurate for the purpose of a study as the present one.

3. Potential heat pump cycles

In this section we introduce four kinds of heat pump cycles all of which having in common the fact that either expansion or compression (whatever is the case) crosses the BZT region in the manner indicated in Fig. 2.

The first heat pump cycle, denoted with HP_1 and introduced in Fig. 3(a), may found applications at heating reactants for performing certain chemical reaction at a desired temperature. The reactants are first preheated and then enter into a constant temperature chemical reactor where endothermic reaction occurs. The hot products exiting the reactor are cooled down with heat recov-

ery. Therefore, the heat delivered to the reactants stream is formed from the heat recovered from the products plus the heat resulted from work conversion in the turbo-compressor. As mentioned in the introduction, and emphasised here again, this scheme makes sense if the work needed to drive the compressor comes from some sort of non-conventional and non-polluting energy source (e.g., wind energy, hydro, nuclear energy etc.).

The thermodynamic cycle has six states. In state 1 there is superheated vapour of BZT fluid. The vapour is compressed and during this process the associated thermodynamic states cross the BZT region. The discharge of the compressor is in the vicinity of the VLE line, in state 2 that is inside the BZT region and such that the BZT effects are exploited at maximum.

In principle the compression process could be conducted near to the line 1–2 illustrated in Fig. 3(a) and the compression is still facilitated because of the feature of the BZT fluid to be easy to compress in that region. At discharge, the vapour is closer to the saturation line than at the suction.

The hot BZT fluid is passed through a coil inside the chemical reactor and delivers heat at constant temperature. The resulting flow in state 3 enters the preheater and cools down to 4. Next, it passes through the throttling valve and is delivered to the boiler at low pressure. The boiling process 5–6 is driven by an external heat source. It follows the preheating of the working fluid with heat recovery from the hot products.

It is to be remarked that the proposed scheme is the opposite of what is common in gas turbine cycles where preheating is never applied at compressor suction. There, the preheating is applied at compressor discharge to improve the cycle efficiency. However, as mentioned above, in the case of heat pumps operating with complex fluids (e.g., BZT) the vapour is easy to compress and one may propose preheating prior to compression. Most gas turbines are designed with cooling channels in their blades. Such experience can be easily transferred to high-temperature turbo-compressors.

The second kind of heat pump, denoted here with HP_2 is introduced with the help of Fig. 3(b): on the left is the pump diagram while on the right side is the associated thermodynamic cycle in *T*–*s* coordinates. The cycle has four states corresponding to four processes. In the state 1 a superheated BZT vapour is admitted into the compressor suction. After compression, the vapour is discharged, similarly to the HP_1 case in state 2, very close to the saturation line. The hot BZT vapour enters the chemical reactor where it assists certain endothermic chemical reaction.

This heat pump configuration may also be found applicable to high-temperature ovens for heat treatments of materials. Many of these ovens in the industry are either fully electrical or operate with fossil fuel (e.g., natural gas). Again, by using heat recovery and converting work from non-conventional sources into heat, the HP_2 cycle presents a cleaner and efficient alternative to replace the traditional electrical or fossil fuel ovens or chemical reactors from industry.

At the exit of the reactor, at state 3, the fluid is a saturated liquid ready to be expanded, in a positive displacement expander allowing for work recovery. A reciprocating expander, a rotating vane expander or other rotating expanders (e.g., scroll, screw) may be used to this purpose, depending on the temperature level. For example, due to their complicated geometry, the maximum operating temperature for screw and scroll machine with current technology is below 300 °C. This threshold may be increased even more by applying cooling of the rotors. Reciprocating and rotating vane expander may be used at even higher temperature because of their simpler geometry that makes easier to account for thermal expansion of the mating mechanical parts.

The heat from the external source is delivered to the working fluid at lowest pressure in the cycle, during the process 4–1 that operates completely in single phase. It is worth noting that because BZT fluids (like siloxanes) are considered extremely stable, and because the process 4–1 is in single phase, this cycle may present good safety for being suitable to nuclear energy.

It is interesting also to remark that the expansion process 3–4 crosses the two-phase region and the expander's discharge is a superheated vapour, while its intake is saturated liquid. Note that this feature enhances the amount of work recovery from the fluid and therefore the cycle efficiency.

In Fig. 3(c) the third heat pump cycle is denoted by HP_3 that operates completely outside the two-phase region. Actually, for the HP_3 and HP_4 cycles (to follow) the BZT effects are exploited in turbine, not in compressor. Heat recovery from the products of the assisted endothermic reaction is assumed to be possible for the case HP_3. As illustrated in the thermodynamic cycle from Fig. 3(c) at the state 1 there is a highly superheated vapour (a BZT gas) that is compressed and discharged at state 2 (also superheated). The heat gained by the working fluid is delivered, non-isothermally, to the chemical reactor. At state 3 there is a supercritical fluid (at temperature and pressure over the critical) which is expanded in a turbine across the BZT region. Work is recovered from the expansion process 3–4. Next the hot products exiting the reactor are used to preheat the working fluid (process 4–1) prior to compressor's suction.

In Fig. 3(d) the HP_4 is presented. This operates after a cycle with state 6. At state 1 the superheated vapour enters the compressor and is discharged at 2. The hot working fluid is delivered to the chemical reactor where it cools down to 3 and releases the desired reaction heat. Next, the fluid passes through a heat recovery heat exchanger and further cools down to 4, from where it is expanded with work recovery during the process 4–5. The external heat source is used to heat the working fluid during the process 5–6, and then the fluid is further heated in the heat recovery heat exchanger, process 6–1. We also note that the heat pump HP_4 is similar to the HP_3 with the exception that the first allows for an increased temperature differential and does not need heat recovery from the products.

4. Performance analysis

Steady state models based on energy balances were elaborated for all proposed heat pump cycles. The four models are similar, and therefore for the sake of not repeating the same information, we describe first the modeling of HP_1. Afterwards, some relevant aspects regarding the modeling of the other heat pump cycles are discussed.

The modeling starts by assuming that the compression process 1–2 evolves with a given isentropic efficiency η_C as

$$\eta_C = \frac{(h_{2s} - h_1)}{(h_2 - h_1)} \tag{3}$$

where h_{2s} represents the enthalpy for isentropic discharge and is calculated with the entropy at state 1 and the discharge pressure at state 2, $h_{2s} = h(s_1, P_2)$.

The enthalpy of the liquid at state 2 is calculated based on the highest pressure in the system, i.e., $P_3 = P_2$ and $h_3 = h'(P_3)$, where "prime" stands for saturated liquid and "double prime" for saturated vapour. Next, one calculates the parameters of state 6 in function of the source temperature (on the working fluid side $T_5 = T_6$), that is the saturation pressure $P_5 = P_6 = P''(T_6)$ and the vapour enthalpy $h_6 = h''(T_6)$. The enthalpy at state 5 corresponds to saturated liquid and is $h_5 = h'(T_5)$. The expansion process in the throttling valve is assumed isenthalpic and thus the enthalpy in state 4 is $h_4 = h_5$. The temperature at state 4 is slightly superior to that at state 5 and given by $T_4 = T(P_4, h_4)$.

The coefficient of performance (COP) of the heat pump is defined as

$$\mathrm{COP} = \frac{(h_3 - h_2)}{(h_2 - h_1)} \tag{4}$$

and the exergetic COP then becomes

$$\mathrm{COP_{ex}} = \mathrm{COP}\left(1 - \frac{T_0}{T_2}\right) \tag{5}$$

indicating that the heat delivered by the heat pump is available at the temperature of the working fluid, namely T_2.

At modeling the HP_2 cycle the thermodynamic state 4 is determined based on the isentropic efficiency of the expander, η_E, which is defined by

$$\eta_E = \frac{(h_3 - h_4)}{(h_3 - h_{4s})} \tag{6}$$

where h_{4s} is the enthalpy corresponding to isentropic discharge, $h_{4s} = h(P_4, s_3)$.

The COP expression for the HP_2 takes in account that there is some work recovery from the expander; therefore one has

$$\mathrm{COP} = \frac{h_3 - h_2}{(h_2 - h_1) - (h_3 - h_4)} \tag{7}$$

and the corresponding exergetic COP is calculated by Eq. (5) as for HP_1.

For calculating the exergetic COP of HP_3 and of HP_4 the average temperature at the sink is considered as $\bar{T} = T_2 + T_3/2$, thus the exergetic COP becomes

$$\mathrm{COP_{ex}} = \mathrm{COP}\left(1 - \frac{T_0}{\bar{T}}\right) \tag{8}$$

Based on the energy balance in the heat recovery heat exchanger, we can write the following equation for the HP_4:

$$(h_3 - h_4) = (h_1 - h_6) \tag{9}$$

One peculiar aspect in the modeling of all heat pumps is represented by determining the location of the BZT region in the T–s thermodynamic diagram and, in function of the case, the discharge state of the compressor or turbine at the very limit of the BZT region. The thermodynamic state 2 is determined in HP_1 and HP_2 cases by an algorithm that calculates the intersection of the $\Gamma = 0$ line with the VLE. This algorithm proceeds as follows:

- It calculates the parameter Γ according to Eq. (1) that is implemented in FluidProp [47] for a range of temperatures in the vicinity of the critical point (the Γ is calculated on the vapour saturation line);
- It determines where Γ changes the sign in the vicinity of the critical point;
- It then uses the bisection method to determine accurately the temperature of the state 2.

The $\Gamma = 0$ line is represented for all cases first in the P–v diagram because there, the line can be expressed as a univocal function $P(v)$, as it can be observed, e.g., in Fig. 1. To do this, for a given specific volume, the pressure interval where the Γ changes sign is found and then bisection method applied to determine corresponding point of the $\Gamma = 0$ locus. After completion of the calculation on the P–v diagram, the $\Gamma = 0$ locus is transposed to the T–s diagram using the following functions implemented in FluidProp [47]: $T = T(P, v)$, $s = s(P, v)$.

For modeling of HP_1 and HP_2 cycles an iterative procedure is applied to solve for the enthalpy at the thermodynamic state 1 such that the discharge of the compressor reaches the imposed thermodynamic state 2. This iteration solves Eq. (3) for h_1; at every step of the iteration the entropy in state 1 is evaluated with $s_1 = s(P_1, h_1)$.

For modeling of HP_3 and HP_4 cycles one chooses the expansion process such that it does not cross the two-phase region. This choice is made because the expander is a turbomachinery (if the expander would be of positive displacement type it is possible to expand over two-phase as in the example of HP_2). Therefore, the first step in the algorithm that determines the process 3–4 (for HP_3) and 4–5 (for HP_4) is to determine the state with maximum entropy on the VLE line.

Next, one determines iteratively the temperature in state 3 such that the thermodynamic state at the discharge of the turbine, operating according to Eq. (6), is on the lowest branch of the $\Gamma = 0$ locus. At the same time, from this iterative algorithm results the pressure at the turbine discharge, i.e., the lowest pressure in the system.

5. Results and discussion

The results are presented in two parts as follows. In the first part graphical results are reported regarding the four types of heat pumps operating with the BZT fluid dodecamethylcyclohexasiloxane, (D_6). These results refer to a parametric study of the four cycles for which the isentropic efficiency of the turbomachinery, the source and sink temperatures are varied in certain ranges. In the second part, relevant parameters are reported for all studied cycles when operating with any of the 17 BZT fluids included in Table 1.

Dodecamethylcyclohexasiloxane (D_6) has been chosen for the first part of the study because it is considered a representative BZT fluid and one could posses a highly accurate thermodynamic model for it [5]. The results presented here for the case of heat pumps with D_6 are qualitatively the same for all other considered BZT fluids. Only for the sake of keeping the paper at a reasonable length we do not include here graphical results with the 16 studied fluids other than D_6. Rather, results for all heat pumps are given in tabulated form for all fluids in the following.

Fig. 4 shows the dependence of COP and the exergetic $\mathrm{COP_{ex}}$ on the isentropic efficiency of the compressor η_C for various pressures at suction. In general the $\mathrm{COP_{ex}}$ is lower than COP because it accounts for the quality of the delivered heat at the sink (its work equivalent) rather than the quantity. The minimum pressure considered in this study is 1 bar. This pressure is safe in the sense that it impedes any water vapour or air from the ambient to enter into the plant circuit and contaminate the working fluid; if this would happen there is danger of fluid decomposition at high-temperature.

The high values of the COP, as compared to common values for heat pumps (COP < 5) are explained by the fact that: (i) the temperature differential (i.e., temperature difference between sink and source) is rather low (~50 °C); (ii) heat recovery from the reactants is used; and (iii) the BZT fluids are easier to compress than the common working fluids (e.g., steam).

In Fig. 5 a similar study for the HP_2 cycle is presented. Additionally, we indicated on this plot, for information only, the saturation temperature corresponding to the saturation pressure for each of the five curves. In order to do the calculations for the plot from Fig. 5 it has been assumed that the isentropic efficiency of the expander is the same as the one of the compressor. Even if this situation may not be found in practice, it is not far from reality, because in case of turbomachinery the efficiency of turbine is only a few percent better than that of a good compressor. The results of the study will not change significantly if a small difference between the two kinds of machines would be assumed. As obtained, in this case the range of COP variation is larger than that of HP_1, but for isentropic efficiency smaller than 0.9 the COP and $\mathrm{COP_{ex}}$ have lower values.

The parametric study referring to HP_3 and HP_4 has been conducted for a fixed (imposed) temperature and a range of pressure at compressor's discharge. The illustration of heat pump cycles construction for this parametric study is shown in Fig. 6 for both sit-

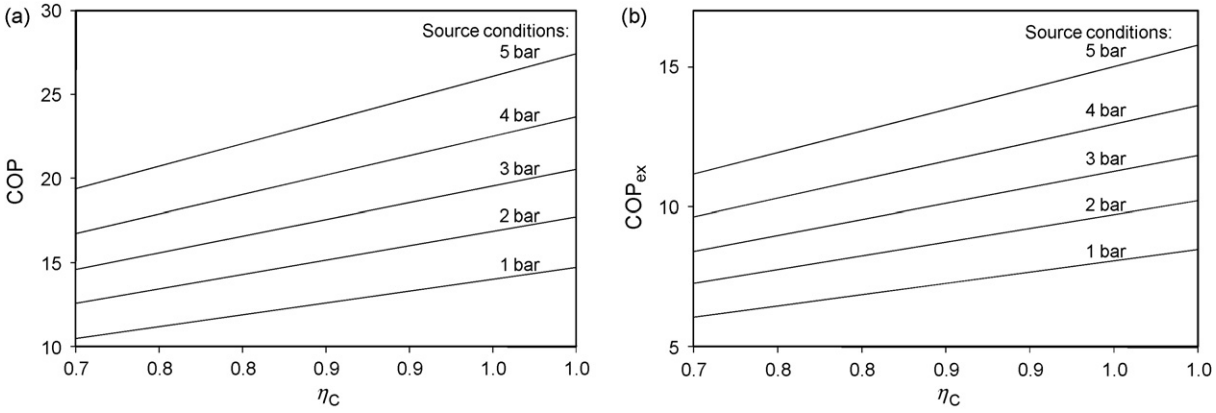

Fig. 4. The COP and COP_{ex} of HP_1 for a practical range of isentropic efficiency.

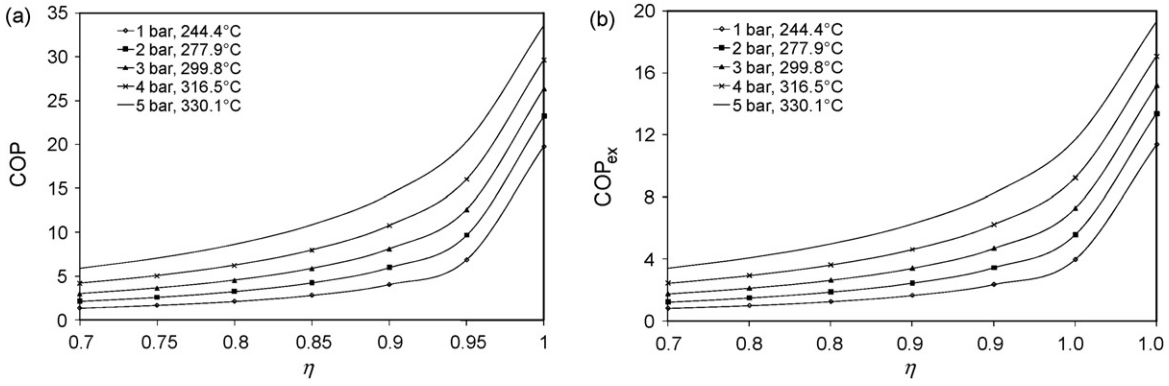

Fig. 5. Variation of the COP and COP_{ex} of HP_2 with isentropic efficiency at various suction pressures.

uations. All the cycles were calculated for an isentropic efficiency of 0.75, which was assumed to be the same for the turbine and the compressor. The suction pressure varies insignificantly from one cycle to another, while the suction temperature variation is remarkable.

The results of this parametric study are presented in Fig. 7 in terms of COP vs temperature at compressor's suction for three values of isentropic efficiency of the (both) turbomachinery. It is interesting to remark that while for HP_3 cycle the COP increases monotonically with T_{suct}, this situation does not stand for HP_4 cycle. Rather in this case for $\eta = 0.9$ one observes a maximum of COP at certain (optimum) T_{suct}. This aspect may be explained by the increase of the compression work with the suction temperature when the process (of compression) is conducted farther from the VLE line. The results regarding COP_{ex} counterpart of this study are presented in Fig. 8.

In what follows we summarize in tabular form the relevant results obtained with the other BZT fluids and D_6. For HP_1 and HP_2 cases the assumed pressure at suction is 1 bar.

The following parameters are presented in Table 2 for the HP_1 cycle: the temperature at compressor discharge, T_{disch}, which is the maximum temperature at the sink, the corresponding pressure P_{disch}, the maximum temperature difference between sink and source $\Delta T_{max} = T_2 - T_6$, the COP and COP_{ex} for two extreme values of the isentropic efficiency of the compressor, namely the lowest considered in the study, $\eta = 0.7$ and the ideal, $\eta = 1$.

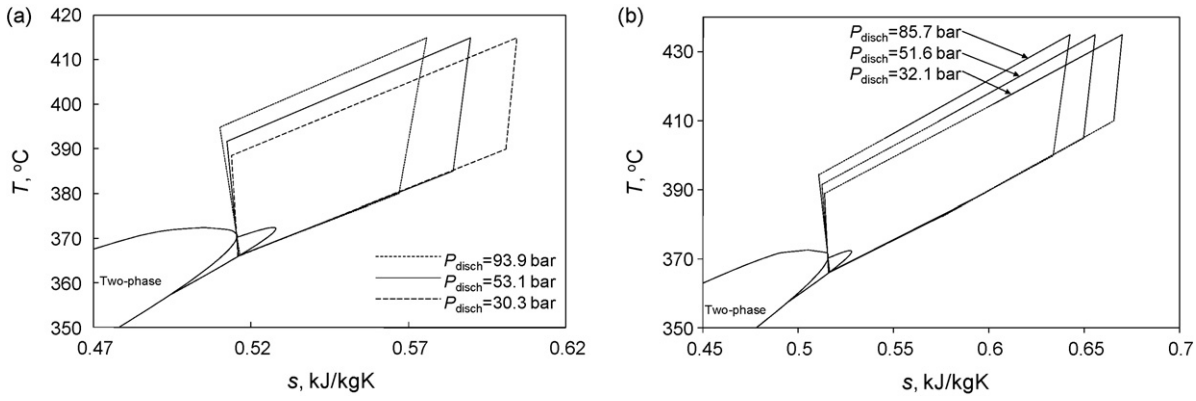

Fig. 6. Thermodynamic cycles HP_3 (a) and HP_4 (b) with compressor's discharge at some temperature and pressure ranges.

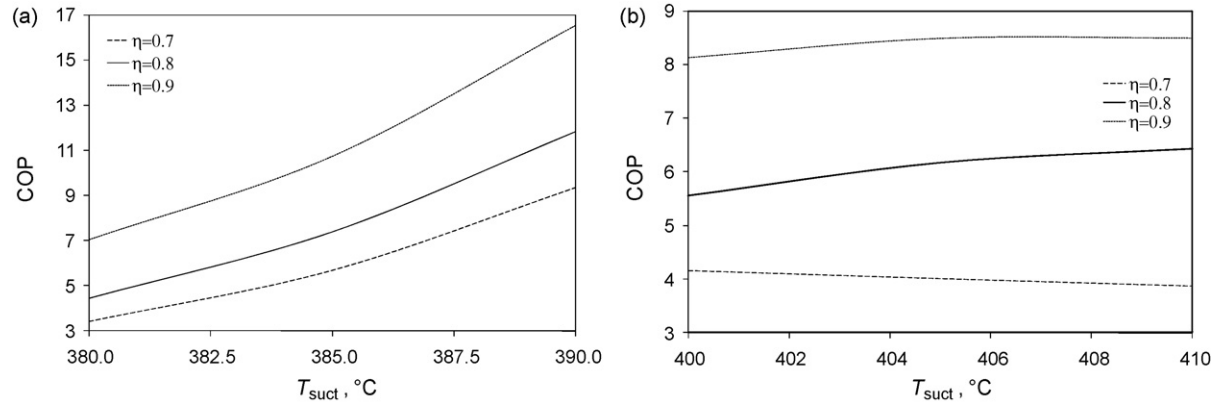

Fig. 7. The COP for HP_3 (a) and HP_4 (b) for a range of suction temperatures at three values of η.

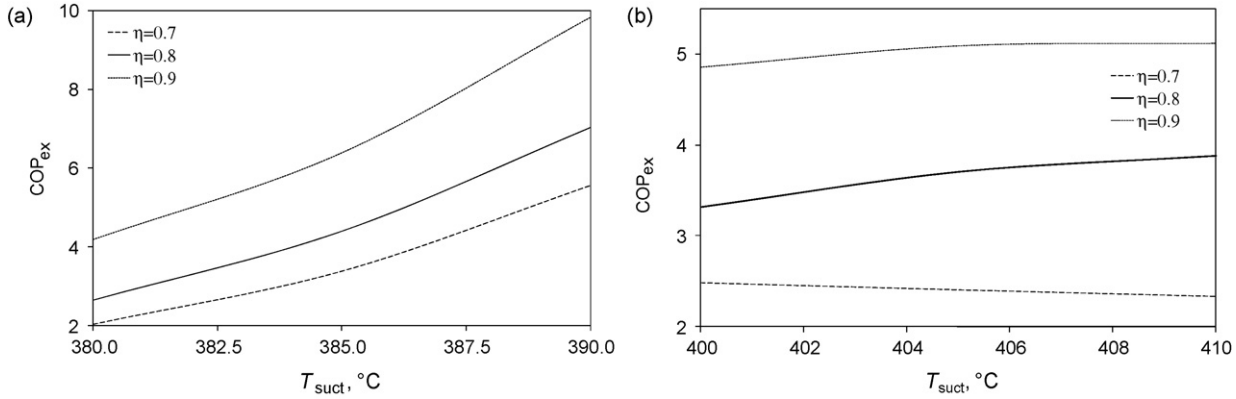

Fig. 8. The COP_{ex} for HP_3 (a) and HP_4 (b) for a range of suction temperatures at three values of η.

Table 2
Relevant parameters for the heat pump cycle HP_1 with selected BZT fluids.

Fluid	D_4	D_5	D_6	MD_3M	MD_4M	MD_5M	MD_6M	PP_5	D_5-D_6	MD_2M-MD_3M	MD_4M-MD_5M	MD_5M-MD_6M
T_{disch} (°C)	307	342	370	352	377	397	414	288	357	338	389	407
P_{disch} (bar)	12.2	11.0	9.3	8.9	8.3	7.4	6.6	16.9	10.0	10.1	8.1	7.0
ΔT_{max} (°C)	133	132	126	107	118	113	106	147	126	123	116	109
$COP_{0.7}$	7.3	8.8	10.5	9.9	11.3	12.6	14.2	6.9	9.7	9.9	11.4	12.5
COP_1	10.1	12.2	14.7	13.8	15.8	17.8	19.9	9.5	13.5	12.9	15.2	16.3
$COP_{ex0.7}$	3.5	4.5	5.6	5.2	6.1	7.0	8.0	3.2	5.5	4.7	5.5	5.9
COP_{ex1}	4.9	6.3	7.9	7.2	8.5	9.9	11.3	4.5	7.7	7.1	8.3	8.7

In Table 3 the results for HP_2 cycle are presented in the same manner as for the HP_1 cycle. One notes only that the temperature differential in this case is $\Delta T_{max} = T_2 - T_4$ and has lower values. The results for the other two heat pumps are compiled in Table 4 and Table 5 respectively. The pressure at suction is also indicated and is about the same for the HP_3 and HP_4 cases. It is mentioned also that, because there is no accurate MH EoS to predict the fluid properties in the liquid phase, the perfluorocarbons PP9, PP10, PP11, PP24 and PP25 were not analyzed for HP_1 and HP_2 cases.

For the discharge temperature and pressure in analysing HP_3 and HP_4, somehow arbitrary supercritical values have been assumed. The only criterion for their choice is to avoid the fluid thermal decomposition. Some data about thermal decomposition of siloxanes are available elsewhere (e.g., [5,24,50]). Based on this

Table 3
Relevant parameters for the heat pump cycle HP_2 with selected BZT fluids.

Fluid	D_4	D_5	D_6	MD_3M	MD_4M	MD_5M	MD_6M	PP_5	D_5-D_6	MD_2M-MD_3M	MD_4M-MD_5M	MD_5M-MD_6M
T_{disch}, (°C)	307	342	370	352	377	397	414	288	357	338	389	407
P_{disch} (bar)	12.2	11.0	9.3	8.9	8.3	7.4	6.6	16.9	10.0	10.1	8.1	7.0
ΔT_{max}, (°C)	49	39	35	39	35	27	24.3	46	43	40	33	26
$COP_{0.7}$	1.3	1.1	1.4	1.5	1.7	1.1	2.8	0.9	1.3	1.4	1.3	1.9
$COP_{0.85}$	2.5	2.2	2.8	3.0	3.4	2.4	5.1	1.8	2.5	2.8	2.7	3.4
COP_1	12.6	16.4	19.8	17.2	20.2	25.7	29.3	12.2	18.0	16.9	18.6	26.0
$COP_{ex0.7}$	0.7	0.6	0.8	0.8	1.0	0.7	1.7	0.4	0.7	0.7	0.9	1.3
$COP_{ex0.85}$	1.0	1.2	1.6	1.7	2.0	1.4	3.1	0.9	1.4	1.5	1.8	2.8
COP_{ex1}	6.7	9.1	11.4	9.7	11.7	15.2	17.7	6.3	10.0	9.3	12.0	16.4

Table 4
Relevant parameters for the heat pump cycle HP_3 with selected BZT fluids.

Fluid	D_4	D_5	D_6	MD_3M	MD_4M	MD_5M	MD_6M	PP_5	PP_9	PP_{10}	PP_{11}	PP_{24}	PP_{25}	D_5-D_6	MD_2M-MD_3M	MD_4M-MD_5M	MD_5M-MD_6M
T_{disch}	357	401	415	400	430	450	470	340	360	410	425	480	450	410	390	440	460
P_{disch}	36.2	34.3	29.2	94.5	25.5	23.0	21.4	52.6	49.7	47.9	43.1	44.3	34.6	29.8	31.1	23.9	22.1
ΔT_{max}	50	59	49	51	53	53	54	52	50	55	50	53	51	53	52	51	53
P_{suct}	12.2	11.0	9.3	8.9	8.3	7.4	6.6	16.9	16.1	15.9	14.3	15.1	11.2	10.0	10.1	8.1	7.0
$COP_{0.7}$	2.7	3.1	3.4	3.0	3.2	3.4	4.0	2.9	3.1	3.1	3.3	3.5	3.6	3.3	2.8	3.1	3.7
COP_1	8.7	9.9	10.8	27.3	27.0	28.1	28.3	11.2	12.0	13.1	13.4	13.9	14.2	10.4	16.7	27.1	28.2
$COP_{ex0.7}$	1.7	1.8	2.0	1.8	2.1	2.3	2.6	1.9	2.0	2.0	2.3	2.7	2.8	1.9	1.7	2.2	2.5
COP_{ex1}	4.7	5.0	6.4	15.9	16.0	16.4	16.9	5.3	5.3	5.7	6.1	6.4	6.5	6.0	15.1	16.3	16.5

Table 5
Relevant parameters for the heat pump cycle HP_4 with selected BZT fluids.

Fluid	D_4	D_5	D_6	MD_3M	MD_4M	MD_5M	MD_6M	PP_5	PP_9	PP_{10}	PP_{11}	PP_{24}	PP_{25}	D_5-D_6	MD_2M-MD_3M	MD_4M-MD_5M	MD_5M-MD_6M
T_{disch}	380	420	435	420	450	470	490	360	410	425	500	470	430	430	410	460	480
P_{disch}	107.0	105.9	86.4	81.1	79.4	68.9	57.3	151.4	146.7	141.3	137.6	139.9	104.2	91.6	93.4	74.3	65.7
ΔT_{max}	70	80	69	70	73	73	74	72	70	75	70	73	71	73	72	71	73
P_{suct}	12.2	11.0	9.3	8.9	8.3	7.4	6.6	16.9	16.1	15.9	14.3	15.1	11.2	10.0	10.1	8.1	7.0
$COP_{0.7}$	3.7	4.0	4.2	4.2	4.4	4.7	4.8	4.0	4.0	4.5	4.6	4.8	4.9	4.1	3.9	4.5	4.7
COP_1	7.2	9.1	10.6	11.1	12.0	12.2	12.5	8.1	8.2	8.4	8.5	8.7	9.0	9.5	11.0	12.1	12.3
$COP_{ex0.7}$	1.3	1.9	2.5	2.7	2.8	3.1	3.6	2.0	2.1	2.3	2.8	2.9	3.0	2.1	2.5	2.9	3.2
COP_{ex1}	3.6	5.0	6.3	6.3	6.5	6.6	7.0	4.1	4.2	4.6	4.6	4.8	4.9	5.5	6.1	6.5	6.7

information, one notes that, in general, couple of tens of degrees above the critical temperature were considered safe for avoiding the thermal decomposition for all fluids.

One may observe from Table 2 that COP and COP_{ex} of the heat pump operating under HP_1 cycle are more "promising" for all selected BZT fluids. The minimum COP value is 6.9, obtained with PP_5 for the lowest isentropic efficiency considered in this study, $\eta_C = 0.7$. There is a reason for this high efficiency: namely heat recovery is applied for heating the working fluid prior to compressor suction, and, both sensible and latent heats delivered at sink are considered to be useful effect.

The situation is however different for the HP_2 cycle since the COP is much lower. In general, an isentropic efficiency of 0.7 for the turbomachinery do not suffice for making this option attractive for most of the BZT fluids analyzed here. Only the heaviest siloxanes MD_6M may be an option, but for very limited applications where a temperature differential as low as ~30 °C is enough. This situation is somehow improved if the isentropic efficiency of the turbomachinery is above 0.85. In this case, siloxanes starting with D_6 may find some potential applications, since they result in COP > 2.4.

The results for the HP_3 and HP_4 cycles show that the efficiency is reasonable only if the isentropic efficiency of turbomachinery is higher than 0.7. Therefore, in that case it is possible to find a limited number of applications of such heat pumps, e.g., as mentioned above for assisting thermo-chemical processes that are suitable for using heat recovery. One has to note however that the temperature differential between source and sink is always small, especially due to the fact the temperature does not increase much at compression of heavy fluids, even if relatively large pressure ratios (e.g., ~10) are used.

6. Concluding remarks

In this paper, we have proposed four kinds of high-temperature heat pumps and studied their performance through energetic and exergetic coefficient of performance with various BZT working fluids for a range of parameters, e.g., isentropic efficiency of turbomachinery and source and sink temperatures. A number of 17 fluids with BZT effects (that may allow in some conditions supersonic compressive flows to propagate isentropically) are identified from the recent literature studies and modeled with the most accurate EoS that are available. All heat pump cycles are designed such that either the expansion or the compression process evolves in the vicinity of VLE line, that is, in a region where non-classical gas dynamics manifest. Moreover, the expansion and hence compression processes are "adjusted" in such a way that maximum benefit from the BZT effect can be obtained, in terms of pressure difference observed across the non-classical gas dynamics region. Thus, the turbomachinery performs with high isentropic efficiency; the higher the turbomachinery efficiency the higher the COP of the heat pump cycle.

Some specific conclusions can also be drawn from this study as:

- The HP_1 cycle may be the most promising because it shows the maximum temperature difference between sink and source, compared to other cycles studied.
- The heat pump HP_2 cycle may present also some good potential, but only if the expander and the turbo-compressor have high isentropic efficiency (>0.85).
- The other heat pump cycles studied here, although they have good COP and COP_{ex}, may find limited applications where small temperature difference between sink and source (30–50 °C) exists.
- The high-temperature heat pumps presented appear to be potential systems, using waste heat, process heat, heat recovered, low-grade heat, etc., which can be employed to reduce the use of fossil fuels and hence the pollution associated with this and provide sustainable energy solution.

Acknowledgements

The authors acknowledge the material support received from the Process and Energy Department at Delft University, The Netherlands, to evaluate the thermophysical properties of the BZT fluids and financial assistance by the Natural Sciences and Engineering Research Council of Canada.

References

[1] A. Kluwick, Theory of shock waves. Rarefaction shocks, in: G. Ben-Dor, O. Igra, T. Elperin, A. Lifshitz (Eds.), Handbook of Shockwaves, vol.1, Academic Press, 2001, pp. 339–411 (Chapter 3.4).
[2] H.A. Bethe, The theory of shock waves for an arbitrary equation of state. Office of Scientific Research and Development, Tech. Rep. (1942) 545.
[3] Y.B. Zel'dovich, On the possibility of rarefaction shock waves, Zh. Eksp. Teor. Fiz. 4 (1946) 363–364.
[4] P.A. Thompson, A fundamental derivative in gas dynamics, Phys. Fluids 14 (1971) 1843–1849.
[5] P. Colonna, A. Guardone, N.R. Nanan, Siloxanes: a new class of candidate Bethe-Zel'dovich-Thompson fluids, Phys. Fluids 19 (2007) 086102.
[6] W.D. Hayes, The basic theory of gasdynamic discontinuities, in: H.W. Emmons (Ed.), Fundamentals of Gas Dynamics, High Speed Aerodynamics and Jet Propulsion, vol. 3, Princeton University Press, Princeton, NJ, 1958.
[7] C. Zamfirescu, A. Guardone, P. Colonna, Admissibility region for rarefaction shock waves in dense gases, J. Fluid Mech. 599 (2008) 363–381.
[8] C. Zamfirescu, P. Colonna, A. Guardone, Maximum wave Mach number of rarefaction shocks in selected BZT fluids, in: HEFAT, 5th International Conference on Heat Transfer, Fluid Mechanics and Thermodynamics, Sun City, South Africa, June, 2007.
[9] C. Zamfirescu, P. Colonna, A. Guardone, Maximum intensity and admissibility region of rarefaction shocks in dense gases. Report ET-2227, Delft University of Technology (2007).
[10] K.C. Lambrakis, P.A. Thompson, Existence of real fluids with negative fundamental derivative, Phys. Fluids 15 (1972) 933.
[11] M.S. Cramer, Negative nonlinearity in selected fluorocarbons, Phys. Fluids A 1 (1989) 1894.
[12] P. Colonna, P. Silva, Dense gas thermodynamic properties of single and multicomponent fluids for fluid dynamics simulations, J. Fluids Eng. 125 (2003) 414.
[13] N.R. Nannan, P. Colonna, C.M. Tracy, R.L. Rowley, J.J. Hurly, Ideal-gas heat capacities of dimethylsiloxanes from speed-of-sound measurements and ab initio calculations, Fluid Phase Equilib. 257 (2007) 102.
[14] P. Colonna, N.R. Nannan, A. Guardone, E.W. Lemmon, Multiparameter equations of state for selected siloxanes, Fluid Phase Equilib. 244 (2006) 193.
[15] G. Angelino, P. Colonna, Multicomponent working fluids for organic Rankine cycles (ORCs), Energy 23 (1998) 449–463.
[16] G. Agelino, C. Invernizzi, Cyclic methylsiloxanes as working fluids for space power cycles, J. Sol. Energ. Trans. ASME 115 (1993) 130–137.
[17] P. Colonna, S. Rebay, Numerical simulation of dense gas flows on unstructured grids with an implicit high resolution upwind Euler solver, Int. J. Numer. Methods Fluids 46 (2004) 735.
[18] D.Y. Peng, D.B. Robinson, A new two-constant equation of state, Ind. Eng. Chem. Fundam. 15 (1976) 59.
[19] R. Stryjek, J.H. Vera, PRSV, An improved Peng-Robinson equation of state for pure compounds and mixtures, Can. J. Chem. Eng. 64 (1986) 323.
[20] P. Colonna, S. Rebay, P. Silva, and T.P. van der Stelt. zFlow: A CFD program using accurate thermodynamic properties of fluids. Software, Delft University of Technology©(2001–2005).
[21] B.P. Brown, B.M. Argrow, Application of Bethe-Zel'dovich-Thompson fluids in organic Rankine cycle engines, J. Propul. Power 16 (2000) 1118.
[22] B.P. Brown, B.M. Argrow, Nonclassical dense gas flows for simple geometries, AIAA J. 36 (1998) 1842–1847.
[23] C. Zamfirescu, A. Guardone, P. Colonna, Preliminary design of the FAST dense gas Ludwieg tube. 9th AIAA/ASME Joint Thermophysics and Heat Transfer Conference, 5–8 June, San Francisco, California, (2006) paper AIAA 2006, p. 3249.
[24] C. Zamfirescu, P. Colonna, R. Nanan, A. Guardone, Experimental options to investigate BZT effects in dense gases. Report ET-2188 Delft University of Technology (2005).
[25] P. Colonna, A. Guardone, N.R. Nannan, C. Zamfirescu, Design of dense gas flexible asymmetric shock tube, J Fluids Eng. 130 (2008), 034501-1-6.
[26] C. Zamfirescu, A. Guardone, P. Colonna, Numerical simulations of the FAST dense gas experiment. European conference on computational fluid dynamics, in: P. Wesseling, E. Oñate, J. Périaux (Eds.), ECCOMAS CFD, ©Delft University of Technology, Netherlands, 2006.
[27] P. Colonna, S. Rebay, J. Harinck, A. Guardone, Real-gas effects in ORC turbine flow simulations: influence of thermodynamic models on flow fields and performance parameters, in: P. Wesseling, E. Oñate and J. Périaux (Eds.), European conference on computational fluid dynamics, ECCOMAS CFD, ©Delft University of Technology, Netherlands, 2006.

[28] P. Cinnella, P.M. Congedo, Aerodynamic performance of transonic Bethe-Zel'dovich-Thompson flows past an airfoil, AIAA J. 43 (2005) 370.
[29] M.F. Orhan, I. Dincer, M.A. Rosen, Environmentally-benign nuclear-based hydrogen production through a copper-chlorine thermochemical cycle, Paper No. 502, in: Proceedings of the Global Conference on Global Warming-2008 (GCGW-08), 6-10 July, Istanbul, Turkey, 2008.
[30] M.A. Lewis, M. Serban, J.K. Basco, Hydrogen production at <550 °C using a low temperature thermochemical cycle, in: Proceedings of Nuclear Production of Hydrogen: Second Information Exchange Meeting, Argonne, Illinois, U.S., 2–3 October, 2003, pp. 145–156.
[31] M. Granowskii, I. Dincer, M.A. Rosen, I. Pioro, Thermodynamic analysis of the use a chemical heat pump to link a supercritical water-cooled nuclear reactor and a thermochemical water-splitting cycle for hydrogen production, J. Power Energy Syst. 2 (2008) 756–767.
[32] M. Granowskii, I. Dincer, M.A. Rosen, I. Pioro, Performance assessment of a combined system to link a supercritical water-cooled nuclear reactor and a thermochemical water splitting cycle for hydrogen production, Energy Conversion Manag. 49 (2008) 1873–1881.
[33] K. Yoshida, Y. Matsumura, H. Morita, Y. Nakahara, A chemical heat pump using hydration of MgO particles in three-phase reactor, Int. J. Energy Res. 19 (1995) 263.
[34] Y. Kato, Y. Yoshizawa, Application of a chemical heat pump to a cogeneration system, Int. J. Energy Res. 25 (2001) 129–140.
[35] H.K. Song, Y.K. Yeo, T.G. Kim, Chemical heat pump based on dehydrogenation and hydrogenation of i-propanol and acetone, Int. J. Energy Res. 16 (1992) 897.
[36] G. Cacciola, V.N. Parmon, Y.I. Aristov, N. Girodano, High-temperature chemical heat pump based on reversible catalytic reactions of cyclohexane-dehydrogenation/benzene-hydrogenation: comparison of the potentialities of different flow diagrams, Int. J. Energy Res. 17 (1993) 293.
[37] M.A. Tahat, R.F. Babushaq, P.W. O'Callaghan, S.D. Probert, Int. J. Energy Res. 19 (1995) 603.
[38] K. Altiniik, T.N. Veziroglu, Metal hydride heat pumps, Int. J. Energy Res. 15 (1991) 549.
[39] K. Abrahamsson, G. Aly, A. Jernquist, S. Stenstrom, Application of heat pump systems for energy conservation in paper drying, Int. J. Energy Res. 21 (1997) 631.
[40] R. Best, F.A. Holland, P.J. Diggory, M.A.R. Eisa, Heat pump assisted distillation. V. A feasibility study on absorption heat pump assisted distillation systems, Int. J. Energy Res. 11 (1987) 179.
[41] R. Jaganathan, P.J. Diggory, S. Supranto, S. Dodda, F.A. Holland, Heat pump assisted distillation. VI. Classified references for heat pump assisted distillation systems from 1945 to February 1986, Int. J. Energy Res. 11 (1987) 327.
[42] O. Ozyurt, O. Comakli, M. Yilmaz, S. Karsli, Heat pump use in milk pasteurization: an energy analysis, Int. J. Energy Res. 28 (2004) 833–846.
[43] L. Itard, Wet compression versus dry compression in heat pumps working with pure refrigerants or non-azeotropic mixtures, Int. J. Refrigeration 18 (1995) 495–504.
[44] C.A. Infante Ferreira, C. Zamfirescu, D. Zaytsev, Twin screw oil-free wet compressor for compression–absorption cycle, Int. J. Refrigeration 29 (2006) 556–565.
[45] P.J. Luickx, L.F. Peeters, L.M. Helsen, W.D. D'haeseleer, Influence of massive heat-pump introduction on the electricitygeneration mix and the GHG effect – Belgian case study, Int. J. Energy Res. 32 (2008) 57–67.
[46] P. Colonna, A. Guardone, Molecular interpretation of nonclassical gas dynamics of dense vapors under the Van der Waals model, Phys. Fluids 18 (2006) 056101.
[47] P. Colonna, T.P. van der Stelt, FluidProp: a program for the estimation of thermo physical properties of fluids, Energy Technology Section, Delft University of Technology, The Netherlands. www.FluidProp.com, 2004.
[48] R. Span, W. Wagner, Equations of State for Technical Applications. I. Simultaneously Optimized Functional Forms for Nonpolar and Polar Fluids, Int. J. Thermophys. 24 (2003) 1–39.
[49] J.J. Martin, Y.C. Hou, Development of an equation of state for gases, AIChE J. 1 (1955) 142–151.
[50] P. Colonna, Fluidi di Lavoro Multi Componenti Per Cicli Termodinamici di Potenza (Multicomponent working fluids for power cycles), Ph.D. thesis, Politecnico di Milano, October (1996).